Metrics for Evaluating the Spatial Accuracy of Microphone Arrays

Daniel Pinardi
Dept. of Engineering and Architecture
University of Parma
Parma, Italy
daniel.pinardi@unipr.it

Angelo Farina
Dept. of Engineering and Architecture
University of Parma
Parma, Italy
angelo.farina@unipr.it

2021 Immersive and 3D Audio: from Architecture to Automotive (I3DA) | 978-1-6654-0998-8/21/$31.00 ©2021 IEEE | DOI: 10.1109/I3DA48870.2021.9610887

Abstract **– The interest in 3D audio is constantly growing, thus leading to the appearance on the market of many microphone arrays for recording spatial audio, having a variety of sizes, number of channels and shapes, mostly spherical. Among the various characteristics that may have an influence on the quality of these systems, the presented work will deal with the spatial accuracy. The availability of robust methods for evaluating the spatial performance of the microphone arrays allows to compare the systems and to study the effect of different geometries, or beamforming algorithms. On one side, the design of new solutions can be optimized, on the other side a user can identify an optimal system depending on his needs. In this paper, two metrics for evaluating the spatial performance of microphone arrays are described, and two common formats for spatial audio are employed, Ambisonics and Spatial PCM Sampling (SPS). In the first part, the parameters Spatial Correlation and Level Difference are used for assessing the accuracy of the Ambisonics format, which is based on Spherical Harmonics functions. In the second part two classic metrics for loudspeakers, i.e., directivity factor and half power beam width, are employed for evaluating the accuracy of unidirectional virtual microphones, which constitute the base of the SPS format. In the last section, four well-known spherical microphone arrays are analyzed and compared through the described metrics and spatial audio formats.**

Keywords—Ambisonics, beamforming, metrics, microphone array, spatial accuracy, Spatial PCM Sampling

I. INTRODUCTION

Ambisonics [1] is probably the most diffused method employed for processing spatial audio. It consists in a Spherical Harmonics (SH) expansion of the pressure signals recorded by the capsules of a microphone array. Systems capable to encode four SH, and usually provided with four capsules, are called First Order Ambisonics (FOA) microphone arrays. If more capsules are available, SH of higher orders can be encoded. Such systems are denoted as High Order Ambisonics (HOA) microphone arrays. In 2010, an alternative spatial audio format was proposed, named Spatial PCM Sampling (SPS) [2], [3] and based on the synthesis of unidirectional virtual microphones aiming in different directions and sampling uniformly the space.

Many microphone arrays are available on the market, with a number of capsules ranging between 4 and 252 [4], [5], [6], [7], [8]. The spatial accuracy of these systems depends on several factors, such as the size, the shape, the position of the capsules and the beamforming algorithm. Hence, the availability of robust metrics for comparing their performance may be particularly useful. Firstly, Ambisonics format is considered, and the parameters Spatial Correlation (SC) and Level Difference (LD), proposed in [9], are employed. Then, two parameters commonly employed for the directivity of sound sources are used for evaluating the SPS format: directivity factor Q [10], [11] and half-power Beam Width BW [12].

Finally, four spherical microphone arrays are analyzed and compared: the Zylia, with 19 capsules and 103 mm diameter, the Eigenmike32™, with 32 capsules and 84 mm diameter, and two arrays by Bruel&Kjaer, both of 195 mm diameter and having 36 capsules and 50 capsules, respectively. Nevertheless, the metrics described in this work can be employed for arrays of any shape [13].

The paper is organized as follow. Section II provides a description of the algorithm and the parameters employed for the beamforming. In section III, the metrics are described, and in section IV the microphone arrays are compared.

II. DEFINITIONS AND THEORY RECALL

When beamforming is performed, the sound pressure signals recorded by the capsules of a microphone array are converted into another set of different signals, which are usually named virtual microphones. Two methods can be used for this conversion, i.e., linear processing and parametric processing. In the first case, a matrix of filters synthesizes the virtual microphones. In the second approach, at first a parametric spatial analysis of the sound scene is performed for extracting the source signals and their locations; then, Ambisonics or SPS formats are recreated using the theoretical formulas, [14], [15], [16], [17], [18].

In this work, a linear encoding approach was employed, and parametric processing will be used in future development. Beamforming is processed with a matrix of Finite Impulse Response (FIR) filters, computed in the frequency domain with a regularized Kirkeby inversion [19]:

$$H_{m,v,k} = \left[C^*_{m,d,k} \cdot C_{m,d,k} + \beta_k \cdot I\right]^{-1} \cdot \left[C^*_{m,d,k} \cdot A_{d,v} \cdot e^{-j\pi k}\right] \quad (1)$$

where $m = [1, \dots, M]$ are the capsules; $v = [1, \dots, V]$ are the virtual microphones; k is the frequency index; $d = [1, \dots, D]$ are the DoA of the sound waves; the matrix C is the complex response of each capsule m for each direction d; the matrix A defines the frequency independent amplitude of the target directivity patterns; $e^{-j\pi k}$ introduces a latency that ensures filters causality; $\cdot$ is the dot product; I is the identity matrix; $[\,]^*$ denotes the conjugate transpose; $[\,]^{-1}$ denotes the pseudo-inverse; β is a frequency-dependent regularization parameter [20]. Depending on the target directivity patterns A, Ambisonics or SPS can be calculated. The resulting matrix H is converted back to the time domain by means of the Inverse Fast Fourier Transform (IFFT), thus obtaining the beamforming matrix h, having dimensions [M;V;N], where N is the length of the filters, that is 8192 in this work.

One can note that the filtering matrix H of (1) is obtained by inverting the matrix C, which is the anechoic spatial response of the array and provides the information of sound pressure on the capsules for many DoA of the sound wave. The matrix C can be obtained with three different approaches: experimental, numerical, and theoretical. The experimental method consists in measuring the microphone array from many directions [21] inside an anechoic chamber, either rotating the microphone array or employing a moving loudspeaker. The numerical method solves the diffraction of the sound waves against the surface of the array in a simulation software, usually employing Finite Elements Method (FEM) or Boundary Elements Method (BEM).

Finally, the theoretical solution, which is the one employed here, consists in solving the analytical equations that describe the interaction between the sound waves and the geometry of the microphone array [22], [23]. It is available only for few cases: plane waves diffracted by a sphere, a cylinder, and a plane [24], [25]. The solution of plane waves diffracted by a rigid sphere was found in [26], however the method and the metrics described in this work can be employed for arrays of any shape, if the matrix C is obtained with the experimental or numerical method. For calculating the matrix C, a set of $D = 240$ directions was employed, arranged in a spherical design, or T-design, of order $T = 21$. Spherical designs are distribution of points, mathematically calculated with recursive method, with the property of maximizing the sampling uniformity over a sphere [27], [28].

For evaluating the beamforming performance of a microphone array, it must be calculated the effective directivity A' obtained with the beamforming for each virtual microphones v in each direction d. This operation is performed by convolving (i.e., multiplying in the frequency domain) the matrix C and the beamforming matrix H:

$$A'_{d,v,k} = \sum_{m=1}^{M} C_{m,d,k} \cdot H_{m,v,k} \tag{2}$$

where $d = [1, \dots, D]$ and $k = [1, \dots, N/2]$. Ideally, i.e., in case of perfect reconstruction, the matrix A' would be frequency independent, thus resulting in $A' = A$ for all the d directions at all frequencies.

The Ambisonics format employed in this work is compliant with the current standard "AmbiX", which defines channel order (ACN) and gain-scaling rules (SN3D) for any Ambisonics order [29]. The coefficients of the target directivity matrix A are those of the SH functions, usually defined as follows [30]:

$$A_{d,v} = \sqrt{\frac{(2n+1)}{4\pi} \frac{(n-v)!}{(n+v)!}} P_n^v(\cos\theta) e^{iv\varphi} \tag{3}$$

where (θ, φ) are the angles of each direction d, respectively elevation and azimuth; n is the degree of the SH, an integer value ≥ 0; v is the order of the SH, comprised in the range $[-n \leq v \leq +n]$; P_n^v are the associated Legendre polynomials [30]. Ambisonics was encoded up to order four for all the microphone arrays compared. Therefore, the filtering matrices H calculated with (1) have dimensions:

- Zylia [19;25;8192]
- Eingemike32™ [32;25;8192]
- Bruel&Kjaer, 36 capsules [36;25;8192]
- Bruel&Kjaer, 50 capsules [50;25;8192]

Differently from Ambisonics, the SPS format does not rely on the SH expansion. Instead, it is an alternative method for capturing the complete spatial information of the sound field, by employing a set of unidirectional microphones distributed to sample uniformly the space. The directivity of these virtual microphones is of type cardioid, of high order and without any side or rear lobes, and it is defined by:

$$A(\vartheta) = [0.5 + 0.5 \cdot \cos(\vartheta)]^n \tag{4}$$

where ϑ is the angle between the aiming direction of the virtual microphone and the DoA of the sound wave; n is the order of the cardioid microphones. The SPS format has been calculated with $V = 32$ and $n = 4$; the directions are those of a spherical design geometry of order $T = 7$. The polar pattern obtained with the described parameters is shown in Fig. 1 and the filtering matrices calculated with (1) have dimensions:

- Zylia [19;32;8192]
- Eingemike32™ [32;32;8192]
- Bruel&Kjaer, 36 capsules [36;32;8192]
- Bruel&Kjaer, 50 capsules [50;32;8192]

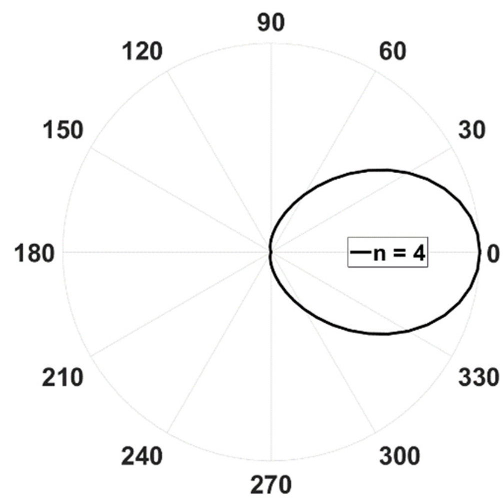

Fig. 1. Polar pattern of a fourth order cardioid microphone employed in the Spatial PCM Sampling format.

III. Definition of the Metrics

A. Ambisonics format

Evaluating the performances of a microphone array in terms of spatial accuracy with Ambisonics format means to estimate the deviation of the virtual microphones A' with respect to the ideal SH. In this work, the metrics described by S. Moreau in [9] have been used: Spatial Correlation (*SC*), defined in (4) and Level Difference (*LD*), defined in (5):

$$SC_{v,k} = \frac{\sum_{d=1}^{D} (A'_{d,v,k})^T \cdot A_{d,v}}{\sum_{d=1}^{D} \left(\sqrt{(A'_{d,v,k})^T \cdot A'_{d,v,k}} \cdot \sqrt{(A_{d,v})^T \cdot A_{d,v}} \right)} \tag{5}$$

$$LD_{v,k} = \frac{1}{D} \sum_{d=1}^{D} \frac{(A_{d,v})^2}{A'_{d,v,k} \cdot (A'_{d,v,k})^*} \tag{6}$$

where $[\ ]^T$ denotes the transpose; A' is the effective directivity of the virtual microphones obtained from (2); A is the target directivity introduced in (1); * denotes the complex conjugate; v are the virtual microphones; d are the directions; k is the frequency. One can note that the metrics are averaged over all the D directions. Then, averaging is applied also among the virtual microphones v belonging to the same Ambisonics order n (ACN standard numbering):

$$SC_{n,k} = \frac{1}{2n+1}\sum_{v=-n}^{n}\left|SC_{v,k}\right| \tag{7}$$

$$LD_{n,k} = -10\log\left[\frac{1}{2n+1}\sum_{v=-n}^{n}LD_{v,k}\right] \tag{8}$$

After averaging, the two parameters depend only on the Ambisonics order and the frequency. Moreau introduced in its equations a vector γ of spatial weightings to compensate for the non-homogeneous distribution of directions around the sphere. Here γ is not required, as the employed distribution, i.e., spherical design, is uniform; (5) and (6) are thus simplified respect to [9].

SC varies in the range $0 \div 1$, while LD varies in the range $-\infty \div +\infty\ [dB]$. Each Ambisonics order is perfectly reconstructed if:

$$SC_{ideal} = 1 \tag{9}$$

$$LD_{ideal} = 0\ [dB] \tag{10}$$

However, a certain amount of error can be accepted. Therefore, in this work the following two ranges of acceptability are employed:

$$SC_{acc.range} = [0.95; 1] \tag{11}$$

$$LD_{acc.range} = [-1; +1]\ [dB] \tag{12}$$

Frequency limits for each order are found considering the most restricted combination provided by the two parameters.

B. Spatial PCM Sampling format

In case of SPS format, the two parameters employed are the Directivity Factor Q and the half-power Beam Width BW. The directivity factor Q is defined as:

$$Q_{[v,k]} = \frac{I_{\max\ [v,k]}}{I_{0\ [v,k]}} \tag{13}$$

where I_{max} is the magnitude of the sound intensity vector in the direction of maximum emission; I_0 is the average of the magnitude of sound intensity over the whole sphere; v is the virtual microphone; k is the frequency.

As shown in Fig. 2, BW is twice the angle of the beam measured between the direction of maximum sensitivity and the direction having gain 3 dB below the maximum:

$$BW_{[v,k]} = 2 \cdot \angle(\vec{S}_{max,[v,k]} - \vec{S}_{max-3\ dB,[v,k]}) \tag{14}$$

where $\vec{S}_{max}$ is the direction of maximum directivity; $\vec{S}_{max-3\ dB}$ is the direction where directivity is reduced by 3dB respect to the maximum; $\angle$ denotes the angle; v is the virtual microphone; k is the frequency.

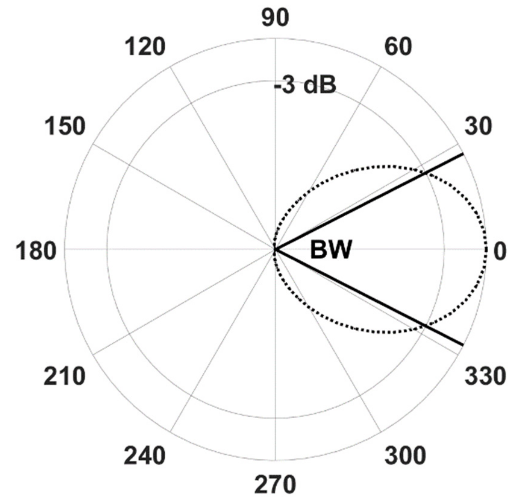

Fig. 2. Definition of the half-power Beam Width (BW).

For a unidirectional virtual microphone, it is desired to have a high value of Q and a low value of BW. The two parameters were calculated in 1/3 octave bands and averaged over all the virtual microphones. The target values of Q and BW were calculated for the SPS format used in this work ($V = 32, n = 4$):

$$Q_{V=32,n=4} = 8.75 \tag{15}$$

$$BW_{V=32,n=4} = 67\ [deg] \tag{16}$$

Also in this case, acceptability tolerances were defined to admit reasonable deviations:

$$Q_{acc.range} = [8.65; 8.85] \tag{17}$$

$$BW_{acc.range} = [65; 69]\ [deg] \tag{18}$$

Frequency limits are found by applying the above acceptance windows and considering the more restricting combination provided by the two parameters.

IV. Spherical Arrays Comparison

The previously described metrics were employed for analyzing the spatial performance of four spherical microphone arrays, the Zylia, the Eigenmike32™ (EM), the Bruel&Kjaer with 36 capsules (B&K-36), and the Bruel&Kjaer with 50 capsules (B&K-50).

A. Ambisonics format

First, the matrix C was obtained for each array, thus the beamforming matrices H were calculated with (1) for the Ambisonics format up to fourth order, and finally the SC and LD metrics were calculated. The curves of each metric are shown superimposed for the various orders. The non-acceptability areas, which are out of the ranges defined in (11) and (12), are darkened in gray. The results are shown in Fig. 3 and Fig. 4 for the Zylia, in Fig. 5 and Fig. 6 for the EM, in Fig. 7 and Fig. 8 for the B&K-36, and in Fig. 9 and Fig. 10 for the B&K-50.

It will be noted that each parameter provides two limits, one at low frequency and one at high frequency, for each order. Therefore, four frequency limits are found; the acceptable frequency range of each order is comprised in the more restrictive limits at low and high frequency. The results for Ambisonics order from 1 to 4 are summarized in TABLE I, TABLE II, TABLE III, and TABLE IV.

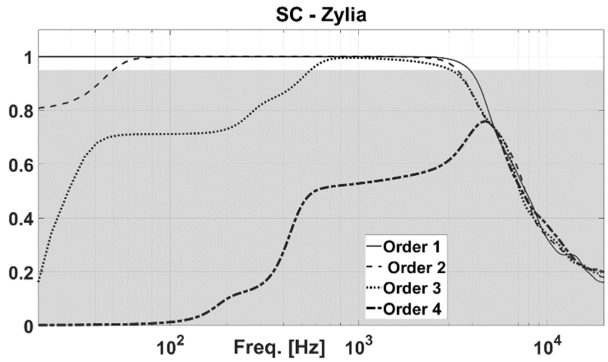

Fig. 3. Zylia, Spatial Correlation metric.

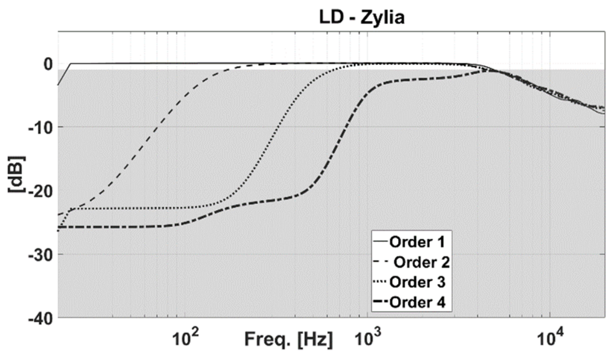

Fig. 4. Zylia, Level Difference metric.

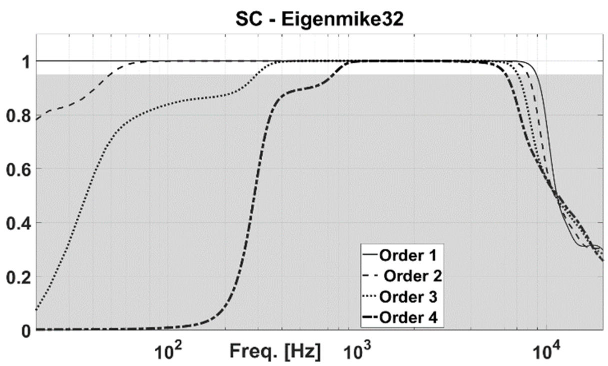

Fig. 5. EM, Spatial Correlation metric.

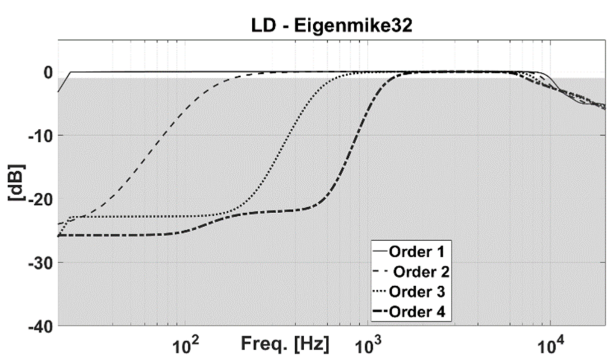

Fig. 6. EM, Level Difference metric.

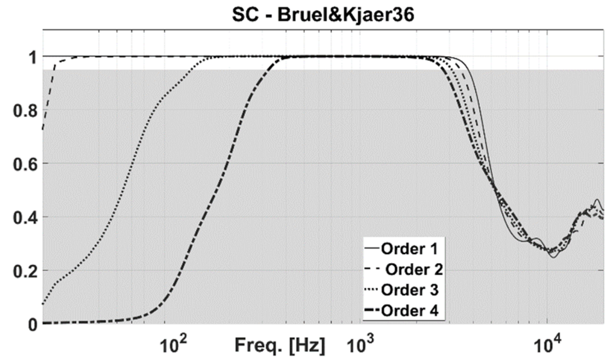

Fig. 7. B&K-36, Spatial Correlation metric.

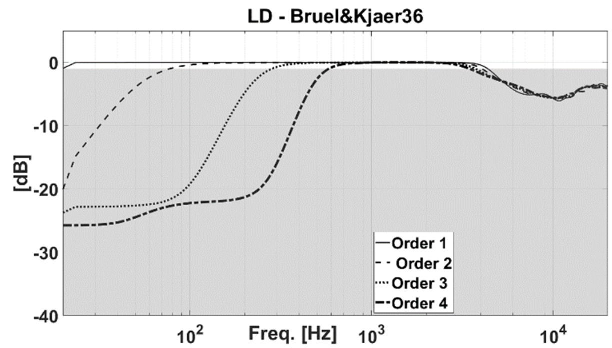

Fig. 8. B&K-36, Level Difference metric.

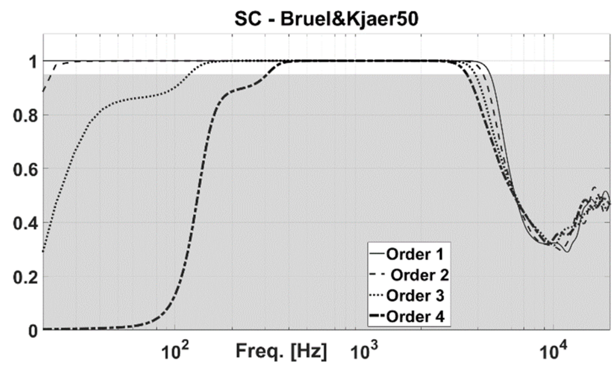

Fig. 9. B&K-50, Spatial Correlation metric.

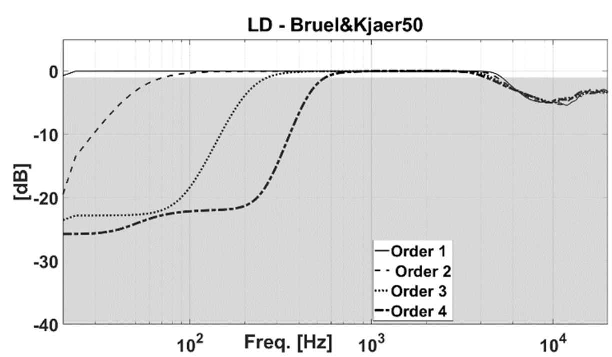

Fig. 10. B&K-50, Level Difference metric.

TABLE I

Ambisonics order 1 – Frequency limits		
Array	**Lower freq. [Hz]**	**Upper freq. [Hz]**
Zylia	20	3870
EM	20	8860
B&K-36	20	3770
B&K-50	20	4630

TABLE II

Ambisonics order 2 – Frequency limits		
Array	**Lower freq. [Hz]**	**Upper freq. [Hz]**
Zylia	170	3330
EM	180	7970
B&K-36	80	3420
B&K-50	70	4260

TABLE III

Ambisonics order 3 – Frequency limits		
Array	**Lower freq. [Hz]**	**Upper freq. [Hz]**
Zylia	660	3080
EM	670	7060
B&K-36	280	3070
B&K-50	260	3860

TABLE IV

Ambisonics order 4 – Frequency limits		
Array	**Lower freq. [Hz]**	**Upper freq. [Hz]**
Zylia	-	-
EM	1370	6100
B&K-36	580	2770
B&K-50	560	3490

To provide a better understanding of the spatial performance of the virtual microphones, some horizontal polar patterns are shown for the EM from Fig. 11 to Fig. 15. The first SH of each order is shown, thus $v = 0, 1, 4, 9$ and 16 following ACN numbering. For each SH, three polar patterns are shown, averaged in octave bands: one at an octave band falling just outside the lower frequency limit given in the tables above, one at $2\,kHz$, a frequency where the polar pattern is correct at any order, and one at $8\,kHz$, which is suboptimal up to 3rd order and wrong at 4th order. The ideal SH (dashed line) is compared with the one obtained from beamforming (continuous line). It is possible to note that the polar plot of the octave band centered at $2\,kHz$ is well matched with the ideal one for all the Ambisonics orders. Instead, at extreme frequencies, the polar plots are smaller (this is the reason why LD curves are reduced by several dB) and distorted (this is the reason why SC is lower than 1).

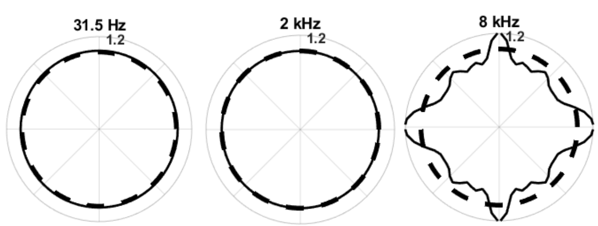

Fig. 11. EM, SH 0 (order 0), 31.5 Hz (left), 2 kHz (center) and 8 kHz (right)

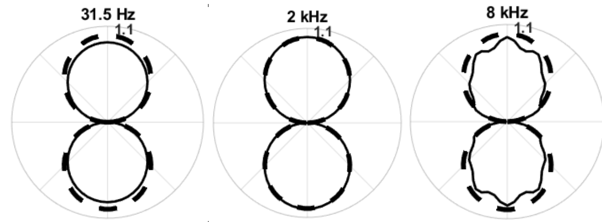

Fig. 12. EM, SH 1 (order 1), 31.5 Hz (left), 2 kHz (center) and 8 kHz (right)

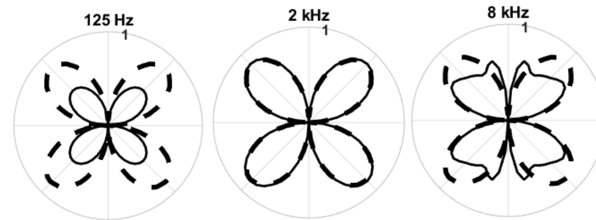

Fig. 13. EM, SH 4 (order 2), 125 Hz (left), 2 kHz (center) and 8 kHz (right)

Fig. 14. EM, SH 9 (order 3), 500 Hz (left), 2 kHz (center) and 8 kHz (right)

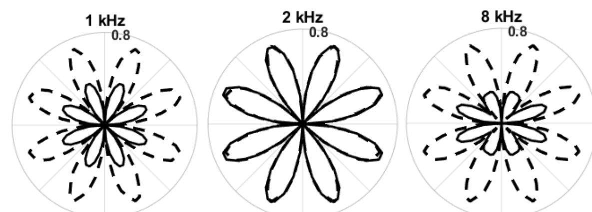

Fig. 15. EM, SH 16 (order 4), 1 kHz (left), 2 kHz (center) and 8 kHz (right)

B. Spatial PCM Sampling format

As in the previous case, the matrix C was obtained for each array, thus the beamforming matrices H were calculated with (1) for the SPS format, and finally the Q and BW metrics were calculated. The curves of each metric are shown superimposed with the theoretical optimal value. The non-acceptability areas, defined by (17) and (18), are darkened in gray. The results are shown in Fig. 16 and Fig. 17 for the Zylia, Fig. 18 and Fig. 19 for the EM, Fig. 20 and Fig. 21 for the B&K-36, and Fig. 22 and Fig. 23 for the B&K-50.

Also in this case, the two parameters provide together four frequency limits, and the acceptable frequency range is comprised in the more restrictive limits at low and high frequency. The results for SPS format are summarized in TABLE V. A good matching between these frequency ranges and those obtained for Ambisonics format is observed.

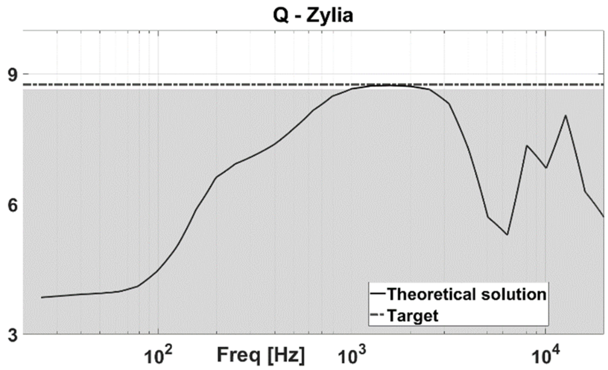

Fig. 16. Zylia, directivity factor Q metric.

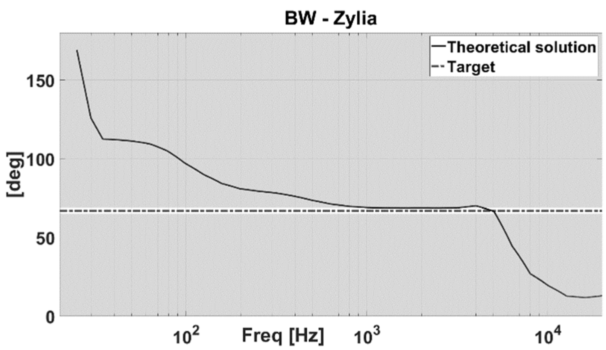

Fig. 17. Zylia, half power beam width BW metric.

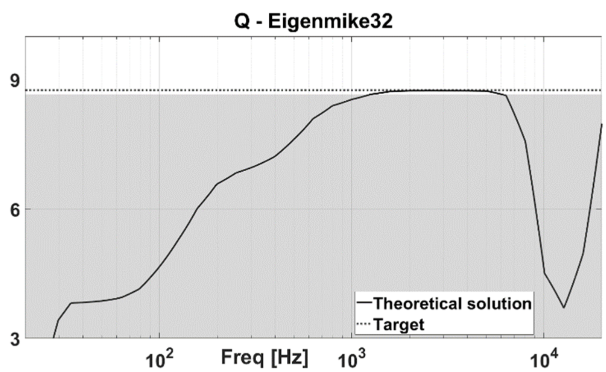

Fig. 18. EM, directivity factor Q metric.

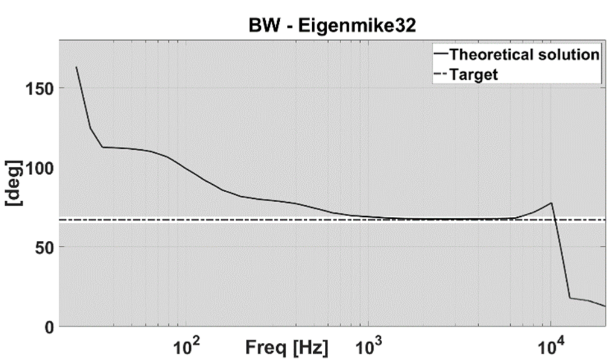

Fig. 19. EM, half power beam width BW metric.

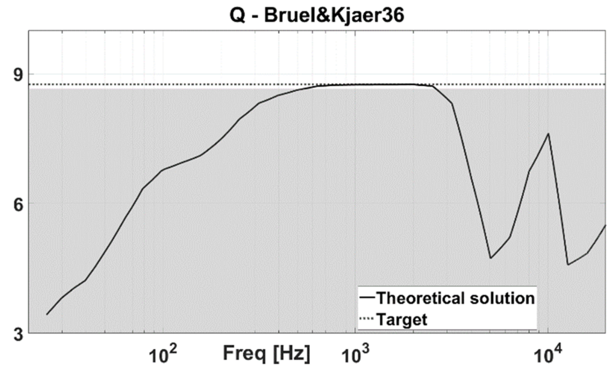

Fig. 20. B&K-36, directivity factor Q metric.

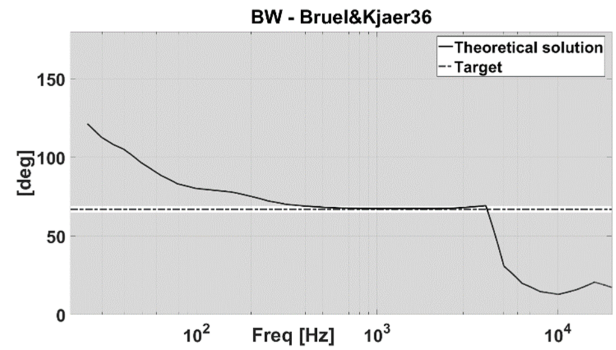

Fig. 21. B&K-36, half power beam width BW metric.

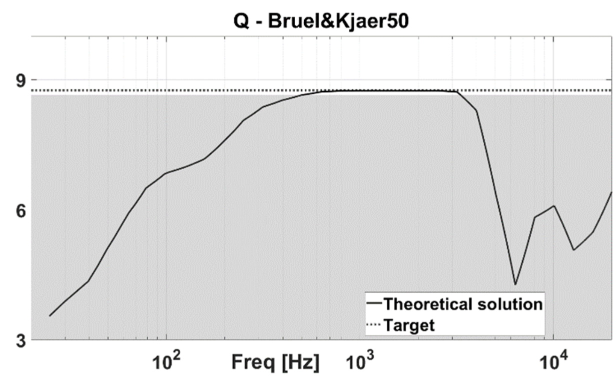

Fig. 22. B&K-50, directivity factor Q metric.

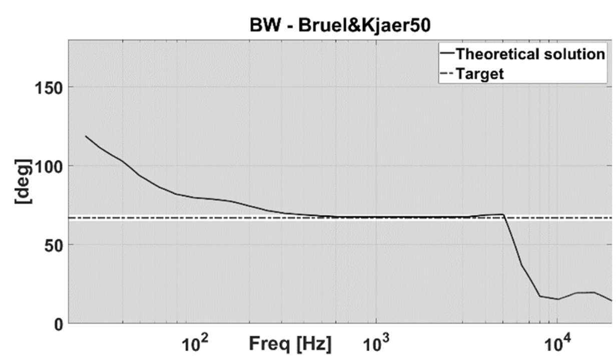

Fig. 23. B&K-50, half power beam width BW metric.

TABLE V

SPS format: V = 32, n = 4		
Array	**Lower freq. [Hz]**	**Upper freq. [Hz]**
Zylia	1000	2500
EM	1240	6110
B&K-36	540	2620
B&K-50	510	3300

Finally, in Fig. 24, Fig. 25, Fig. 26, and Fig. 27 the horizontal polar patterns of the SPS virtual microphones shown, superimposing the target directivity (dashed line) with the one obtained from beamforming (continuous line). In this case, three polar plots are shown for each microphone array: one at an octave band centered in a suboptimal low frequency range, one at the octave band centered at 2 kHz and one at an octave band centered in a suboptimal high frequency range. It is possible to note that the polar plot of the octave band centered at 2 kHz is well matched with the ideal one for all the microphone arrays. This condition corresponds to the flat central part of the curves Q and BW: Q is in a local maximum and BW is in a local minimum. Instead, at suboptimal frequencies, the polar plots are distorted.

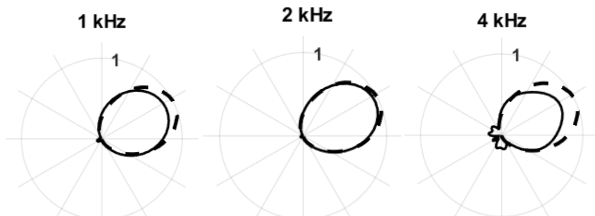

Fig. 24. Zylia, fourth order virtual cardioid, 1 kHz (left), 2 kHz (center) and 4 kHz (right).

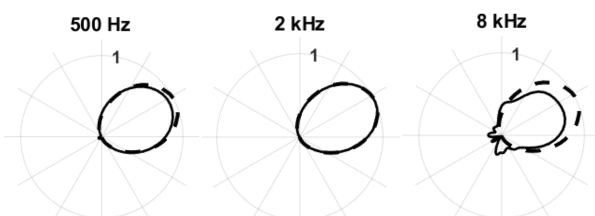

Fig. 25. EM, fourth order virtual cardioid, 500 Hz (left), 2 kHz (center) and 8 kHz (right).

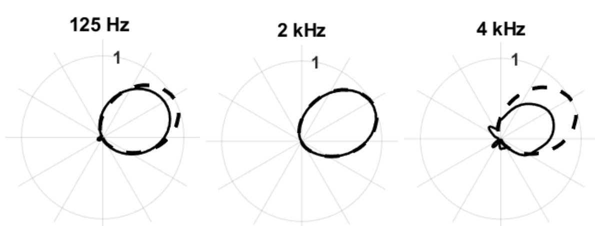

Fig. 26. B&K-36, fourth order virtual cardioid, 125 Hz (left), 2 kHz (center) and 4 kHz (right).

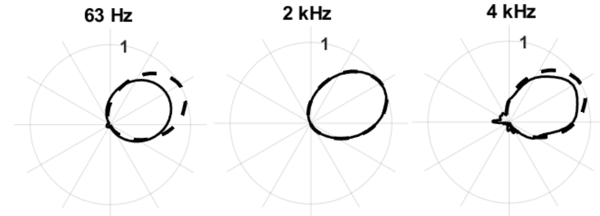

Fig. 27. B&K-50, fourth order virtual cardioid, 63 Hz (left), 2 kHz (center) and 4 kHz (right).

V. Conclusions

The Spatial Correlation and Level Difference parameters proposed by S. Moreau have been taken up for assessing the Ambisonics spatial audio format. Then, two parameters commonly employed for the directivity of sound sources have been used for assessing the Spatial PCM Sampling format: directivity factor (Q) and half-power Beam Width (BW). Acceptability thresholds were defined for each metric, allowing to estimate the frequency ranges of optimal beamforming of the microphone arrays.

In the second part of the paper, the spatial performance of four existing spherical microphone arrays, i.e., Zylia, Eigenmike32™, and Bruel&Kjaer with 36 and 50 capsules were analyzed. The anechoic response of the arrays, required to solve the beamforming algorithm, were calculated theoretically, thus relying on the analytical solution of plane waves diffracted by a rigid sphere. The analysis was performed with both spatial audio format, thus fourth order Ambisonics, and Spatial PCM Sampling with 32 virtual cardioid microphones of order four.

Finally, a further evidence of the results obtained with the analysis of the metrics was provided, by comparing the polar patterns of the virtual microphones with the target functions, which have an ideal directivity, in three octave bands. In case of Ambisonics, the first SH of each order from zero to four was shown for the Eigenmike32™. In case of SPS, one virtual microphone (fourth order cardioid) was shown for each array. It was provided evidence that an almost perfect agreement between encoded and ideal directivity is found within the optimal frequency range defined by the metrics. Conversely, in the octave bands centered at frequencies below and above the acceptable range, deviations between the encoded directivities and the target functions are clearly visible, coherently with the metrics described.

References

[1] M. A. Gerzon, "Periphony: With-height Sound Reproduction," *Journal of the Audio Engineering Society,* vol. 21, pp. 2-10, 1973.

[2] A. Farina, M. Binelli, A. Capra, E. Armelloni, S. Campanini and A. Amendola, "Recording, Simulation and Reproduction of Spatial Soundfields by Spatial PCM Sampling (SPS)," *International Seminar on Virtual Acoustics,* 2011.

[3] A. Farina, A. Amendola, A. Capra and C. Varani, "Spatial analysis of room impulse response captured with a 32-capsules microphone array," in *130th AES Conference*, 2011.

[4] N. M. Ferres, "An Elementary Treatise on Spherical Harmonics and Subjects Connected with them," *London: Macmillan and Co.,* 1877.

[5] A. Farina, A. Capra, L. Conti, P. Martignon and F. Fazi, "Measuring spatial impulse responses in concert halls and opera houses employing a spherical microphone array," *19th International Congress On Acoustics,* September 2007.

[6] N. Peters and A. W. Schmeder, "Beamforming using a spherical microphone array based on legacy microphone characteristics," *Proc. of the International Conference on Spatial Audio (ICSA),* 2011.

[7] S. Sakamoto, S. Hongo, T. Okamoto, Y. Iwaya and Y. Suzuki, "Sound-space recording and binaural presentation system based on a 252-channel microphone array," *Acoustical Science and technology,* vol. 36, no. 6, pp. 516 - 526, 2015.

[8] J. Meyer and G. Elko, "A highly scalable spherical microphone array based on an orthonormal decomposition of the soundfield," *Proc. on IEEE International Conference on Acoustics, Speech and Signal Processing (ICASSP),* vol. 2, pp. 1781 - 1784, 2002.

[9] S. Moreau, J. Daniel and S. Bertet, "3D sound field recording with higher order ambisonics-objective measurements and validation of spherical microphone," *120th AES Convention,* 2006.

[10] C. Coleman, An Introduction to Radio Frequency Engineering, Cambridge University Press, 2004.

[11] B. Rafely, Fundamentals of Spherical Array Processing, Springer-Verlag Berlin Heidelberg, 2015.

[12] H. L. V. Trees, Optimum Array Processing, John Wiley & Sons, 2004.

[13] D. Pinardi, "A Human Head Shaped Array of Microphones and Cameras for Automotive Applications," in *I3DA - International Conference on Immersive and 3D Audio*, Bologna, 2021.

[14] S. Delikaris-Manias and V. Pulkki, "Parametric Spatial Filter Utilizing Dual Beamformer and SNR-Based Smoothing," in *AES 55th International Conference: Spatial Audio*, 2014.

[15] V. Pulkki, "Directional audio coding in spatial sound reproduction and stereo upmixing," in *Proc. 28th AES International Conference*, Pitea, 2006.

[16] V. Pulkki, "Spatial Sound Reproduction with Directinal Audio Coding," *Journal of the AES,* vol. 55, no. 6, pp. 503-516, 2007.

[17] S. Berge and N. Barrett, "High Angular Resolution Planewave Expansion (HARPEX)," in *Proc. of the 2nd International Symposium on Ambisonics and Spherical Acoustics*, 2010.

[18] V. Pulkki, A. Politis, M. V. Laitinen, J. Vilkamo and J. Ahonen, "First-order directional audio coding (DirAC)," in *Parametric Time-Frequency Domain Spatial Audio*, 2017, pp. 89-138.

[19] O. Kirkeby, F. Orduna, P. A. Nelson and H. Hamada, "Inverse filtering in sound reproduction," *Measurement and Control,* vol. 26, no. 9, pp. 261 - 266, November 1993.

[20] H. Tokuno, O. Kirkeby, P. A. Nelson and H. Hamada, "Inverse filter of sound reproduction systems using regularization," *IEICE Transactions on Fundamentals of Electronics, Communications and Computer Sciences,* Vols. E80-A, no. 5, pp. 809 - 820, 1997.

[21] A. Farina, A. Capra, L. Chiesi and L. Scopece, "A Spherical Microphone Array for Synthesizing Virtual Directive Microphones in Live Broadcasting and in Post Production," *40th International Conference: Spatial Audio: Sense the Sound of Space,* 2010.

[22] L. McCormack, S. Delikaris-Manias, A. Farina, D. Pinardi and V. Pulkki, "Real-time conversion of sensor array signals into spherical harmonic signals with applications to spatially localised sub-band sound-field analysis," *144th AES Convention,* 2018.

[23] L. McCormack, S. Delikaris-Manias, A. Politis, D. Pavlidi, A. Farina, D. Pinardi and V. Pulkki, "Applications of spatially localized active-intensity vectors for sound-field visualization," *Journal of the Audio Engineering Society,* vol. 67, no. 11, pp. 840-854, 2019.

[24] J. W. S. Rayleigh, The Theory of Sound - Volume II, New York: Dover Publications, 1896.

[25] R. O. Duda and W. L. Martens, "Range dependence of the response of a spherical head model," *Journal of Acoustical Society of America,* vol. 104, no. 5, pp. 3048-3058, 1998.

[26] A. Politis, "Acoustical Spherical Array Processing Library," Department of Signal Processing and Acoustics, Aalto University, Finland, 2016. [Online]. Available: http://research.spa.aalto.fi/projects/spharrayproc-lib/spharrayproc.html#59.

[27] R. H. Hardin and N. J. A. Sloane, "McLaren's Improved Snub Cube and Other New Spherical Designs in Three Dimensions," *Discrete and Computational Geometry,* vol. 15, pp. 429-441, 1996.

[28] D. Pinardi, "Spherical t-Designs for Characterizing the Spatial Response of Microphone Arrays," in *I3DA - International Conference on Immersive and 3D Audio*, Bologna, 2021.

[29] C. Nachbar, F. Zotter and E. Deleflie, "Ambix - A suggested Ambisonics format," *Ambisonics Simposium,* 2011.

[30] E. G. Williams, Fourier Acoustics: Sound Radiation and Nearfield Acoustical Holography, Academic Press, 1999.

D. Pinardi received the M.S. (Cum Laude) degree in Mechanical Engineering from University of Parma, Italy, in July 2016, with a thesis on loudspeaker modelling. In March 2020, he got the Ph.D. degree in industrial engineering with a thesis on the design of microphone, hydrophone, and camera arrays for spatial audio recording.

He is a research assistant of Prof. Angelo Farina from 2016, mainly specialized in spatial audio. Topics of his interest are design of sensors arrays, simulations and auralization, applied to automotive field and underwater acoustics.

Angelo Farina got his M.S. degree in civil engineering in December 1982 at the University of Bologna, Italy, with a thesis on the acoustics and vibrations inside a tractor cab. In 1987, he got a Ph.D. in Technical Physics at the University of Bologna with at thesis on experimental assessment of concert hall acoustics. He was a full-time researcher since 1st November 1986 at the University of Bologna and since 1st march 1992 at the University of Parma. He became Associate Professor on 1st November 1998 and he is Full Professor of Environmental Applied Physics since 1st May 2005 at the University of Parma, where he has the chair of Applied Acoustics and Technical Physics.

During his academic career, Angelo worked in several fields of Applied Acoustics, including noise and vibration, concert hall acoustics, simulation software and advanced measurement systems. In the last 10 years, he focused mostly on applications involving microphone and loudspeaker arrays. In 2008, Angelo Farina was awarded with the AES fellowship for his pioneering work on electroacoustic measurements based on exponential sine sweeps.

Angelo is author of more than 250 scientific papers and three widely employed software packages (Ramsete, Aurora plugins, DISIA).